

## **General Disclaimer**

### **One or more of the Following Statements may affect this Document**

- This document has been reproduced from the best copy furnished by the organizational source. It is being released in the interest of making available as much information as possible.
- This document may contain data, which exceeds the sheet parameters. It was furnished in this condition by the organizational source and is the best copy available.
- This document may contain tone-on-tone or color graphs, charts and/or pictures, which have been reproduced in black and white.
- This document is paginated as submitted by the original source.
- Portions of this document are not fully legible due to the historical nature of some of the material. However, it is the best reproduction available from the original submission.



# ANALYTICAL STUDY OF THERMAL BARRIER COATED FIRST STAGE BLADES IN F100 ENGINE

(NASA-CR-135359) ANALYTICAL STUDY OF  
THERMAL BARRIER COATED FIRST-STAGE BLADES IN  
AN F100 ENGINE Progress Report, 1 Sep. 1977  
- 31 Jan. 1978 (Pratt and Whitney Aircraft)  
27 p HC A03/MF A01

N78-17058

Unclas  
04460

CSCI 21E G3/07

UNITED TECHNOLOGIES CORPORATION  
PRATT & WHITNEY AIRCRAFT GROUP  
GOVERNMENT PRODUCTS DIVISION

Prepared for

NATIONAL AERONAUTICS AND SPACE ADMINISTRATION

NASA Lewis Research Center  
Contract No. NAS 3-21032



|  |  |  |  |
|--|--|--|--|
| 1. Report No.<br>NASA CR-135359  | 2. Government Accession No.  | 3. Recipient's Catalog No.                                 |  |
| 4. Title and Subtitle<br>AN ANALYTICAL STUDY OF THERMAL<br>BARRIER COATED FIRST-STAGE<br>BLADES IN AN F100 ENGINE  |  | 5. Report Date<br>February 1978                            | 6. Performing Organization Code  |
|  |  | 8. Performing Organization Report No.<br>FR-9609           | 10. Work Unit No.  |
| 7. Author(s)<br>D. E. Andress  | 9. Performing Organization Name and Address<br>United Technologies Corporation<br>Pratt & Whitney Aircraft Group<br>Government Products Division<br>West Palm Beach, Florida 33402 |  | 11. Contract or Grant No.<br>NAS 3-21032   |
| 12. Sponsoring Agency Name and Address<br>National Aeronautics and Space Administration<br>Washington, D.C. 20546  |  |  | 13. Type of Report and Period Covered<br>Contractor Report 1 September 1977<br>through 31 January 1978 |
| 15. Supplementary Notes<br>Project Manager, Mr. J. Merutka,<br>NASA Lewis Research Center,<br>Cleveland, Ohio  |  |  |  |
| 16. Abstract<br><br>Heat transfer and stress analyses were performed on two sections of a Thermal Barrier Coated (TBC) F100 1st-stage turbine blade. Results of the analyses indicate that the TBC on the leading edges of both sections experience the highest elastic strain ranges and these occur during transient engine operation. Further study is recommended to determine the effects of plastic deformation (creep) and creep-fatigue interaction on coating life. |  |  |  |
| 17. Key Words (Suggested by Author(s))<br><br>Thermal Barrier Coatings<br>Cooled Turbine Blades  |  | 18. Distribution Statement<br><br>Unclassified — Unlimited |  |
| 19. Security Classif. (of this report)<br>Unclassified   | 20. Security Classif. (of this page)<br>Unclassified   | 21. No. of Pages<br>33                                     | 22. Price*   |

## FOREWORD

This report was prepared by the Government Products Division of Pratt & Whitney Aircraft Group, United Technologies Corporation under Contract No. NAS 3-21032, "An Analytical Study of Thermal Barrier Coated First Stage Blades in an F100 Engine." The program was administered by Mr. J. Merutka of the Lewis Research Center, National Aeronautics and Space Administration, Cleveland, Ohio. The work was performed under the direction of D. E. Andress, P&WA Program Manager. This is the final report for the program and covers the technical work accomplished during the period 1 September 1977 through 31 January 1978.

PRECEDING PAGE BLANK NOT FILMED.

## CONTENTS

| <i>Section</i> |  | <i>Page</i> |
|----------------|--|-------------|
| I              | SUMMARY.....                           | 1           |
| II             | INTRODUCTION.....                      | 2           |
| III            | DESCRIPTION OF ANALYSIS.....           | 3           |
|                | Model Description.....                 | 3           |
|                | Analysis.....                          | 5           |
| IV             | RESULTS AND DISCUSSION OF RESULTS..... | 8           |
| V              | CONCLUSIONS AND RECOMMENDATIONS.....   | 19          |
|                | APPENDIX — MATERIAL PROPERTIES.....    | 20          |

PRECEDING PAGE BLANK NOT FILMED

## ILLUSTRATIONS

| <i>Figure</i> |   | <i>Page</i> |
|---------------|---|-------------|
| 1             | Bill-of-Material First-Stage Turbine Blade Showing Sections Analyzed.....   | 3           |
| 2             | F100(3) Thermal Barrier Coated First-Stage Blade — 10% Span Section, Finite Element Model.....                            | 4           |
| 3             | F100(3) Thermal Barrier Coated First-Stage Blade — Midspan, Finite Element Model.....                                     | 5           |
| 4             | Typical F100 Cycle.....   | 6           |
| 5             | F100(3) Thermal Barrier Coated First-Stage Blade — 10% Span Section, Adiabatic Wall Temperature Distribution.....         | 9           |
| 6             | F100(3) Thermal Barrier Coated First-Stage Blade — Midspan, Adiabatic Wall Temperature Distribution.....                  | 10          |
| 7             | F100(3) Thermal Barrier Coated First-Stage Blade — 10% Span Section, External Heat Transfer Coefficient Distribution..... | 11          |
| 8             | F100(3) Thermal Barrier Coated First-Stage Blade — Midspan, External Heat Transfer Coefficient Distribution.....          | 12          |
| 9             | F100(3) Thermal Barrier Coated First-Stage Blade — 10% Span, Temperature vs Surface Distribution.....                     | 13          |
| 10            | F100(3) Thermal Barrier Coated First-Stage Blade — Midspan, Temperature vs Surface Distribution.....                      | 14          |
| 11            | F100(3) Thermal Barrier Coated First-Stage Blade — 10% Span, Surface Strain vs Time.....                                  | 15          |
| 12            | F100(3) Thermal Barrier Coated First-Stage Blade — Midspan, Surface Strain vs Time.....                                   | 16          |
| 13            | F100(3) Thermal Barrier Coated First-Stage Blade — 10% Span, Strain vs Temperature.....                                   | 17          |
| 14            | F100(3) Thermal Barrier Coated First-Stage Blade — Midspan, Strain vs Temperature.....                                    | 18          |
| A-1           | Thermal Conductivity.....   | 20          |
| A-2           | Specific Heat.....  | 21          |
| A-3           | Elastic Modulus.....  | 21          |
| A-4           | Thermal Coefficient of Linear Expansion.....  | 22          |
| A-5           | Ceramic Layer Fracture Strain $Y_2O_3ZrO_2$ .....   | 22          |



## **SECTION I**

### **SUMMARY**

An analytical investigation was conducted to determine the effects of having a Thermal Barrier Coating on F100 first stage turbine blades. Heat transfer and elastic stress analyses were performed at two spanwise locations, 10% and 50% span. Both out-of-plane and in-plane elastic stress analyses were conducted. Maximum strain ranges were calculated for the coating during a typical F100 transient cycle. Results of the analyses show that the highest strain ranges in the coatings occurred at the leading edges of both spanwise locations. The magnitudes of these strain ranges were then compared with that allowed for the coatings. Based on the limited data available, the coating would be expected to fail essentially over all areas of the airfoil. Because this has not been observed in previously-tested blades, it is recommended that the blades be examined to determine the possibility of micro-cracking, which could provide stress relief for the ceramic while allowing it to remain attached to the blade. Further study is also recommended to determine the effects of plastic deformation (creep) and creep-fatigue interaction on coating life and to define thermal fatigue properties of the zirconia coating material.

## SECTION II

### INTRODUCTION

As part of the Full-Scale Engine Research (FSER) test program being conducted at NASA-Lewis, thermal barrier coatings for turbine blades are being evaluated in an F100 engine. The blades are covered by a 10-mil yttria-stabilized zirconia ( $ZrO_2-Y_2O_3$ ) protective coating over a 3-mil NiCrAlY bond coat. The blades were coated by NASA using the plasma spray process. To date the thermal barrier coated blades have accumulated approximately 10 hours run time without visible damage.

A design analysis was required to determine if engine results are predictable and to acquire a more comprehensive understanding of the coating performance during actual operating conditions. The purpose of this study was to provide the results of heat transfer and stress analyses of two spanwise locations on the blade. These results will then be compared with FSER test data when it becomes available.

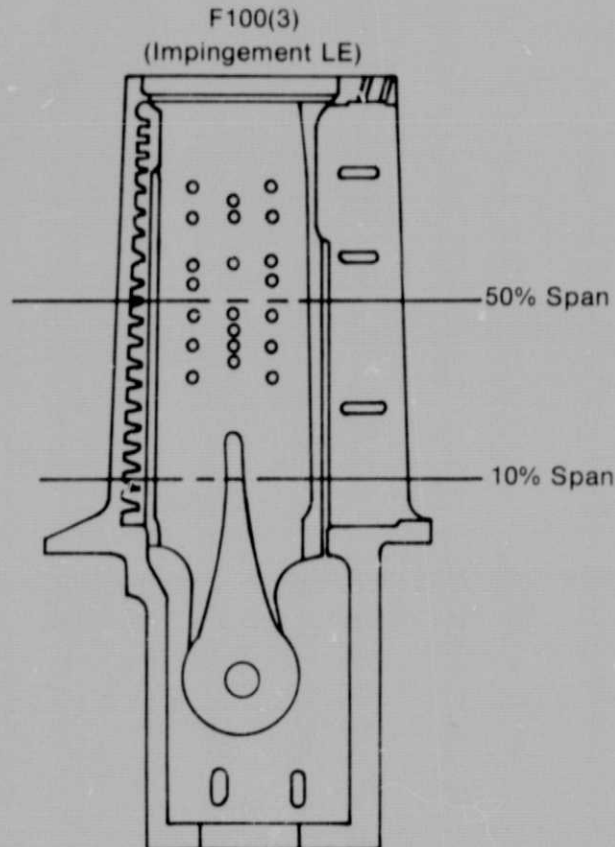


### SECTION III

### DESCRIPTION OF ANALYSIS

#### MODEL DESCRIPTION

The analysis described in this report was conducted on the F100 first blades coated by NASA under the Full Scale Engine Research (FSER) program with an yttria-stabilized zirconia thermal barrier coating (TBC). The F100 blade is a directionally-solidified MAR-M-200 (PWA 1422) casting. The blade is cooled by impingement/convection techniques with coolant discharge through a pedestal trailing edge (Figure 1). Leading edge impingement and midchord convection is implemented by a tip-inserted, cast cooling tube that is pinned at the root. Heat transfer and elastic stress analyses were performed at two spanwise locations, 10% and 50% span. Previously-tested TBC blades showed that the 10% span section was undamaged while the 50% section showed considerable distress. Thus, an attempt was made to predict this difference analytically. The 2-D finite element breakups used in the analyses are shown in Figures 2 and 3, including breakups of the 3-mil NiCrAlY and 10-mil TBC layers.



FD 127070

Figure 1. Bill-of-Material First-Stage Turbine Blade Showing Sections Analyzed

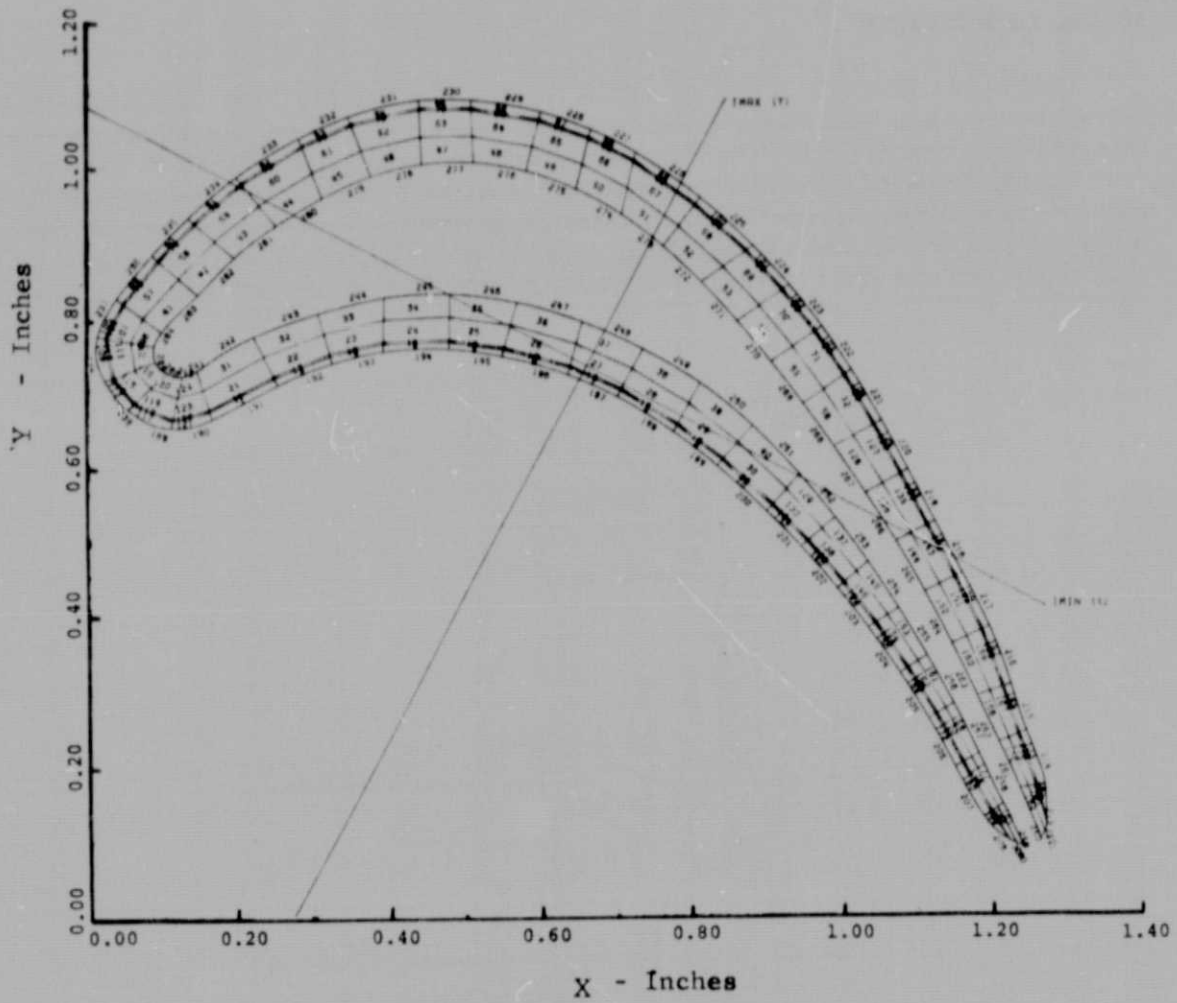


Figure 2. F100(3) Thermal Barrier Coated First-Stage Blade —  
10% Span Section, Finite Element Model

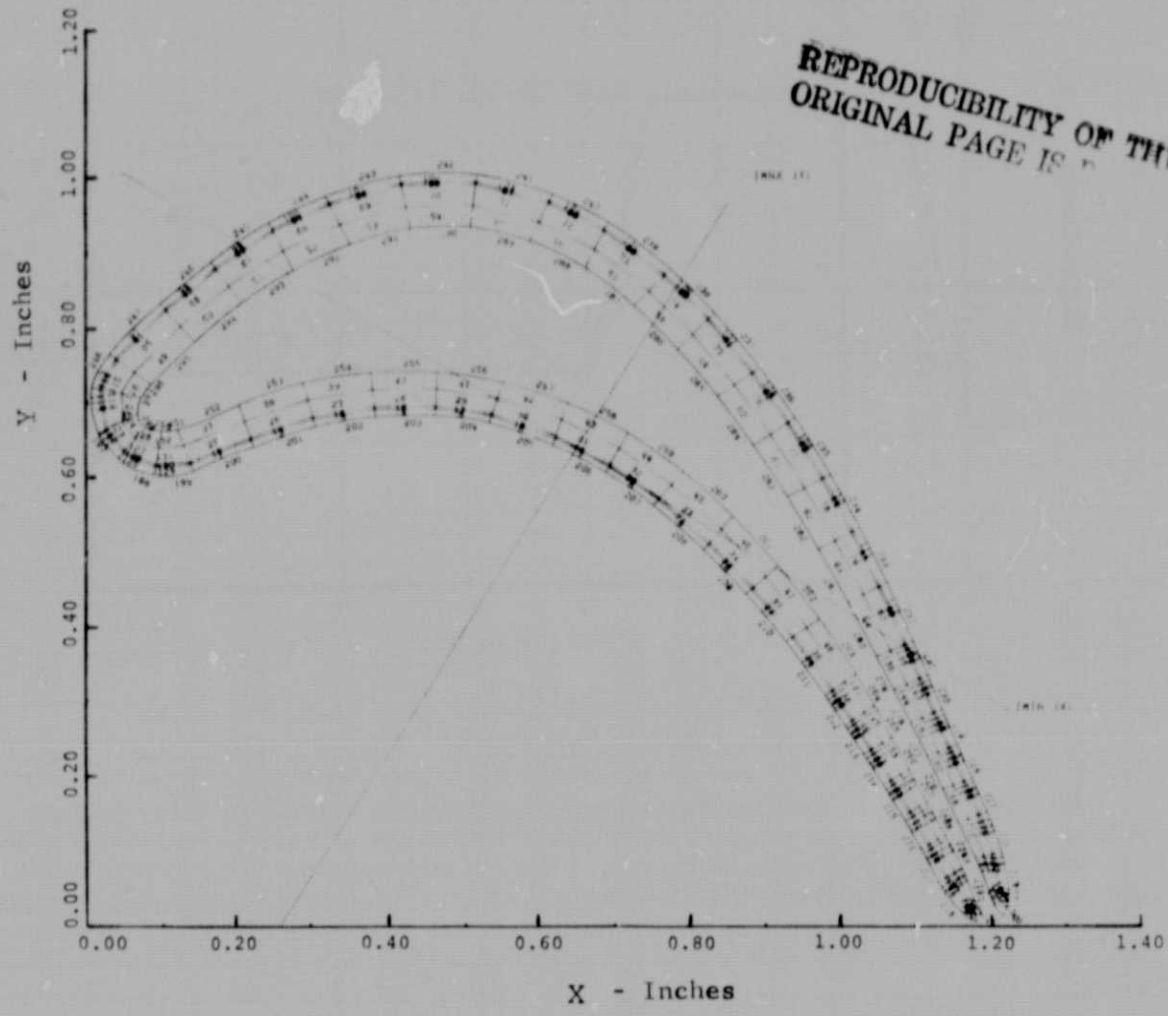


Figure 3. F100(3) Thermal Barrier Coated First-Stage Blade — Midspan, Finite Element Model

**ANALYSIS**

Transient and steady-state heat transfer and elastic stress analyses were performed on the 10% and 50% span cross-sections of a thermal barrier coated first blade for a typical F100 engine cycle as defined in Figure 4. These spanwise locations were selected for two reasons: (1) based on observations of previously-tested JT9D-7F coated blades, the 10% and 50% span locations represented areas of unfailed and failed coating respectively, and (2) analytical studies of these sections without thermal barrier coating were available for comparison.

External heat transfer coefficients and adiabatic wall temperatures were determined using a P&WA-developed computer program which simultaneously accounts for the behavior of both the velocity and temperature boundary layers on an airfoil. Secondary flow effects were accounted for in the determination of adiabatic wall temperature. Coolant side heat transfer coefficients and temperatures were calculated using a compressible flow program which accounts for pressure drop and temperature change due to rotation, friction, heat transfer, and sudden changes in cross-sectional area.

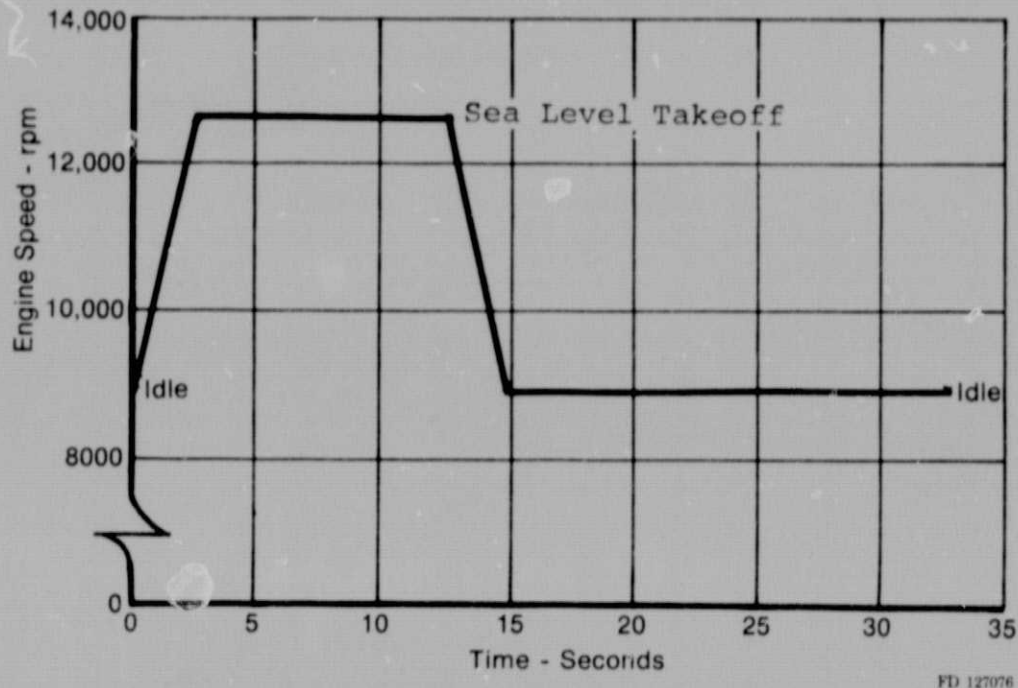


Figure 4. Typical F100 Cycle

After application of a ceramic thermal barrier coating over a NiCrAlY coated metal airfoil, residual stresses exist in the ceramic coating and airfoil because of the differences in thermal expansion. The metal shrinks more than the ceramic as both cool down from the application temperature of several hundred degrees to room temperature, thus inducing compressive stresses in the coating. The effects of these residual stresses were accounted for in the analysis by the use of a stress-free temperature ( $T_{SF}$ ) as the reference temperature instead of room temperature, which is normally used. For the stress analysis an effective coefficient of linear expansion was defined as follows:

$$\alpha_e = \frac{\alpha (T - 70) - \alpha_{SF} (T_{SF} - 70)}{(T - T_e)}$$

where  $\alpha$  and  $\alpha_{SF}$  are the coefficients based on room temperature and evaluated at  $T$  and  $T_{SF}$ . Based on testing previously conducted at P&WA the stress-free temperature was calculated to be 700°F. This value was used in the analysis described in this report.

A generalized heat transfer and elastic stress analysis program was used to determine the airfoil transient and steady-state metal temperature distributions and strain ranges for coating life evaluation. Both in-plane and out-of-plane analyses were performed. The in-plane and out-of-plane strains were combined to determine an effective out-of-plane strain using the following equation:

$$\epsilon_z = \frac{1}{E} \left[ \sigma_z - \nu (\epsilon_x + \sigma_y) \right]$$

where

$\epsilon_z$  = effective out-of-plane strain

E = elastic modulus

$\nu$  = Poisson's ratio

$\sigma_{x,y,z}$  = stresses from in-plane and out-of-plane analyses.

These effective strains were used to determine the maximum strain range in this coating during the engine cycle.

This maximum strain range and associated temperature were then used to predict coating failure. Material properties used in this analysis are shown in Figures A-1 through A-5 in the Appendix.

## SECTION IV

### RESULTS AND DISCUSSION OF RESULTS

The calculated external boundary conditions (adiabatic wall temperatures and heat transfer coefficients) are shown in Figures 5 through 8 for 10% span and 50% span sections, respectively.

Figures 9 and 10 show the calculated airfoil coating surface temperature distributions. Comparisons of average metal temperature are also shown for coated and uncoated blades, showing reductions of 96° and 124°, respectively, for the 10% and 50% span sections. After accounting for the additional centrifugal pull stress of the added coating, these reductions could be converted to a savings of approximately 1.2% in first blade cooling air and still maintain current average metal temperatures.

Figures 11 and 12 show the calculated elastic strain range histories for the leading edge and pressure surface, where distress had been observed previously, and the location of maximum heat flux on the suction side of the 10% and 50% span sections. The minimum strain occurs at 2.0 seconds into acceleration and the maximum strain occurs at 1.5 seconds into deceleration. These values are shown in the table below along with the associated coating temperatures. Maximum strain range is defined as the difference between minimum and maximum strain. These are shown graphically as a function of temperature in Figures 13 and 14 for the two spans analyzed. At these temperatures and strain ranges Bill-of-Material aluminide coatings would be expected to fail.

ELASTIC STRAINS FOR 10% AND 50% SPAN SECTIONS  
AT SEA LEVEL TAKEOFF (STEADY STATE),  
ACCELERATION, AND DECELERATION

|                       |                      | <i>10 Percent Span Section</i> |                |                      |
|-----------------------|----------------------|--------------------------------|----------------|----------------------|
|                       |                      | <i>Suction Side</i>            | <i>Leading</i> | <i>Pressure Side</i> |
|                       |                      | <i>Mid-Chord</i>               | <i>Edge</i>    | <i>Trailing Edge</i> |
| SLTO (S.S.)           | $\epsilon_{max}$ (%) | 0.06                           | 0.36           | 0.226                |
|                       | Temp (°F)            | 1754                           | 1849           | 1715                 |
| DECEL<br>(T=13.5 sec) | $\epsilon_{max}$ (%) | 0.484                          | 0.53           | 0.395                |
|                       | Temp (°F)            | 1254                           | 1135           | 1321                 |
| ACCEL<br>(T=2.5 sec)  | $\epsilon_{max}$ (%) | -0.107                         | -0.20          | 0.036                |
|                       | Temp (°F)            | 1382                           | 1591           | 1254                 |
|                       |                      | <i>50 Percent Span Section</i> |                |                      |
| SLTO (S.S.)           | $\epsilon_{max}$ (%) | 0.11                           | 0.13           | 0.329                |
|                       | Temp (°F)            | 2011                           | 2219           | 1783                 |
| DECEL<br>(T=13.5 sec) | $\epsilon_{max}$ (%) | 0.388                          | 0.60           | 0.479                |
|                       | Temp (°F)            | 1450                           | 1346           | 1408                 |
| ACCEL<br>(T=2.5 sec)  | $\epsilon_{max}$ (%) | -0.218                         | -0.29          | 0.072                |
|                       | Temp (°F)            | 1576                           | 1921           | 1266                 |



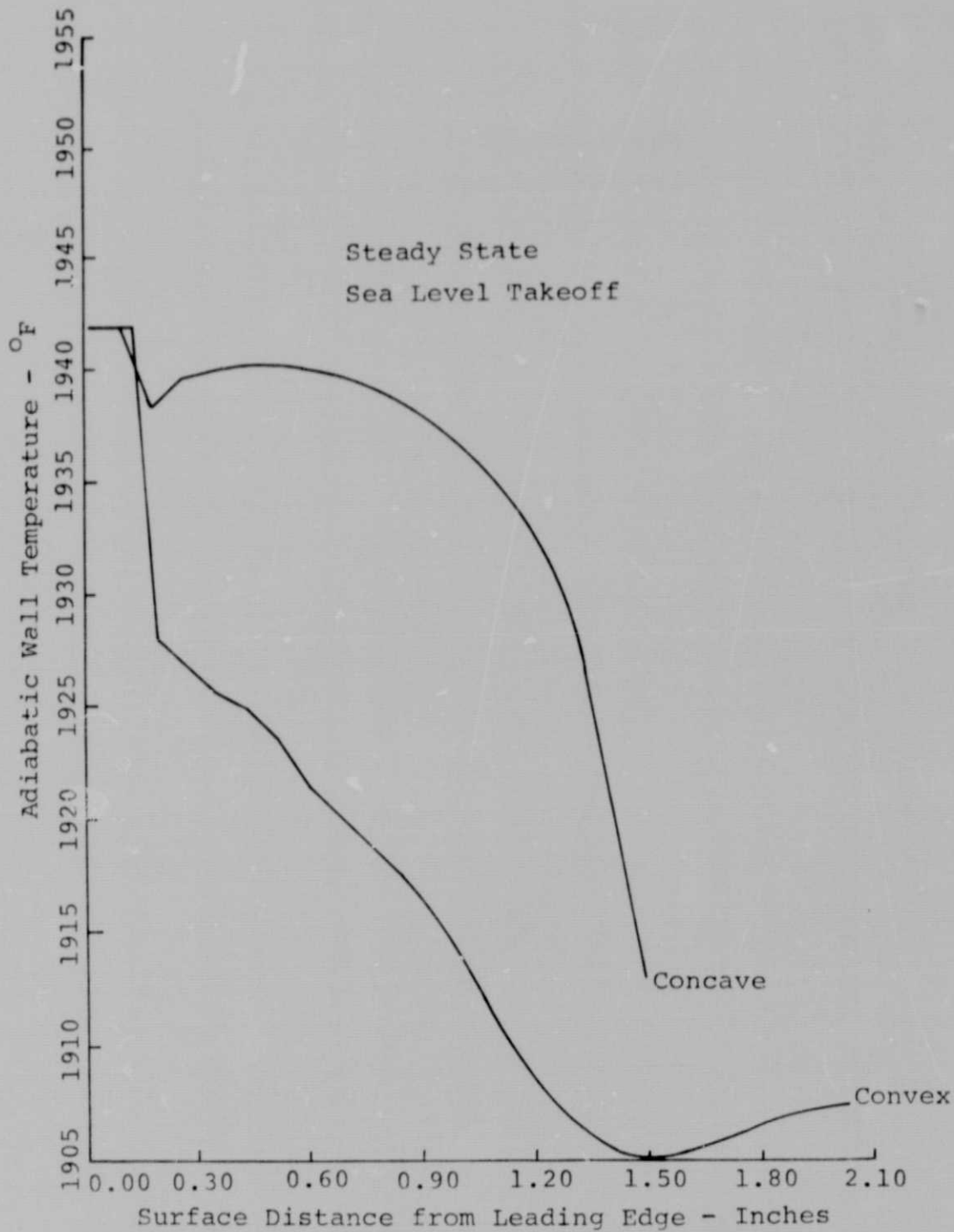


Figure 5. F100(3) Thermal Barrier Coated First-Stage Blade —  
10% Span Section, Adiabatic Wall Temperature  
Distribution

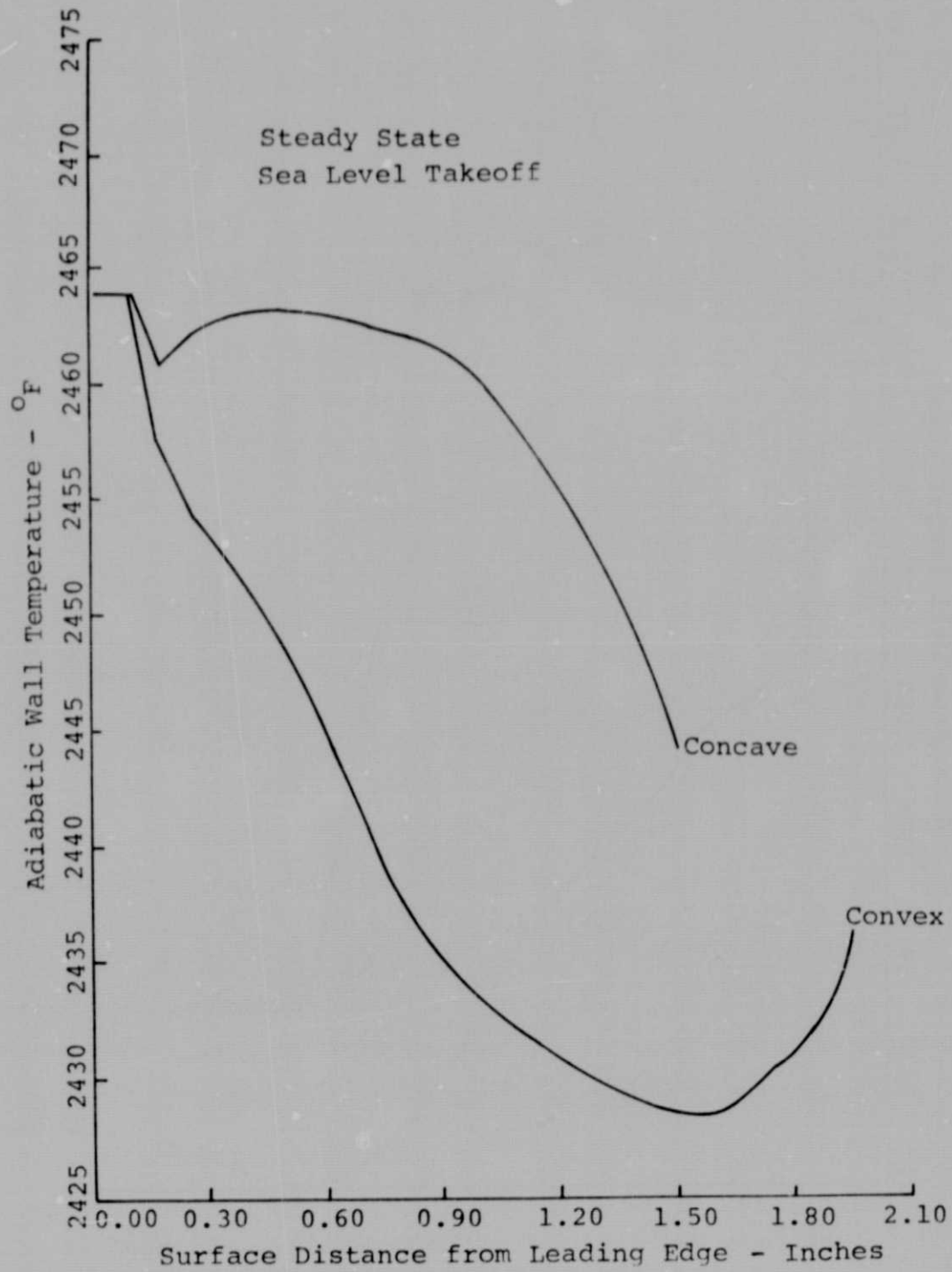


Figure 6. F100(3) Thermal Barrier Coated First-Stage Blade —  
Midspan, Adiabatic Wall Temperature Distribution

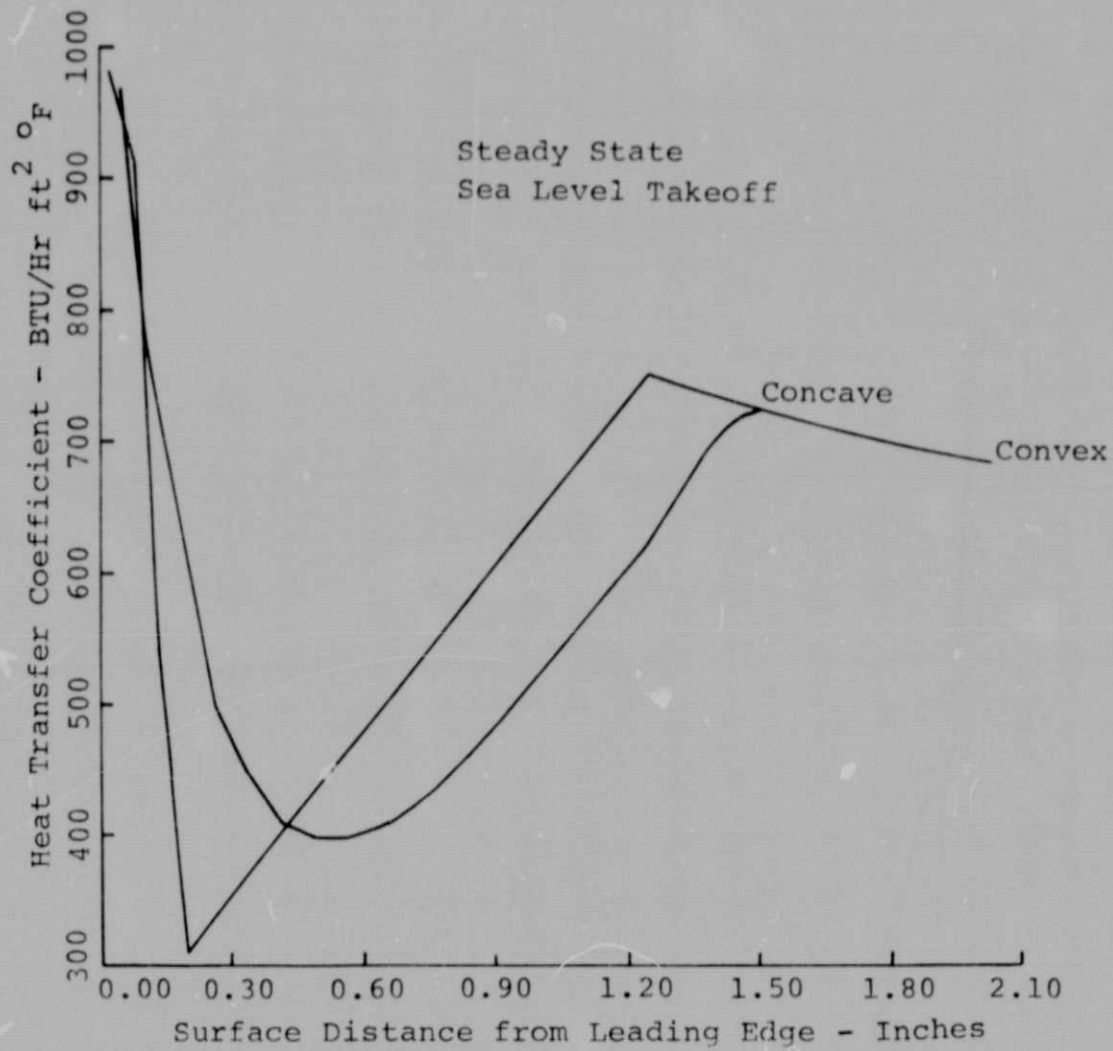


Figure 7. F100(3) Thermal Barrier Coated First-Stage Blade —  
10% Span Section, External Heat Transfer Coefficient  
Distribution

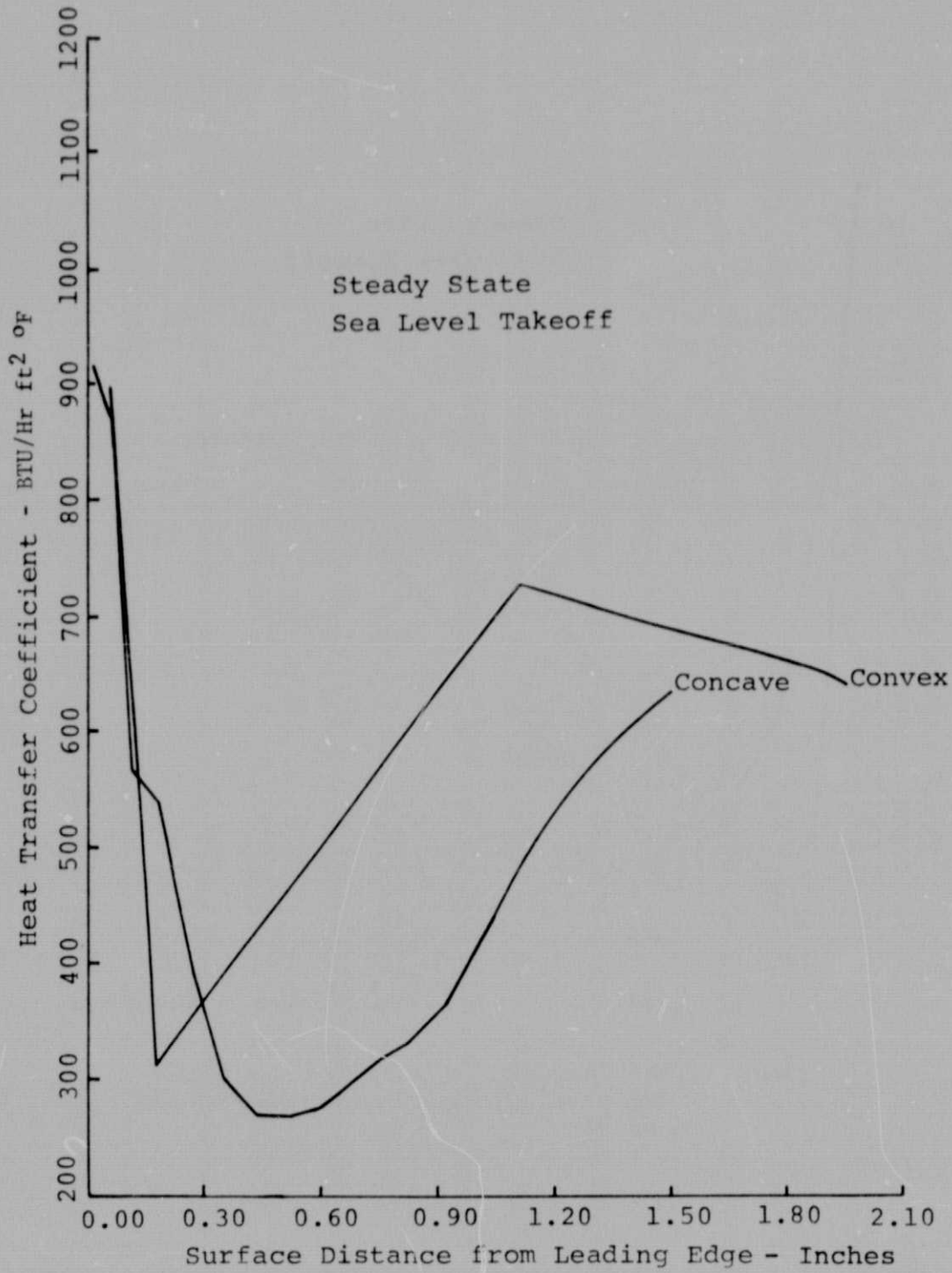


Figure 8. F100(3) Thermal Barrier Coated First-Stage Blade — Midspan, External Heat Transfer Coefficient Distribution

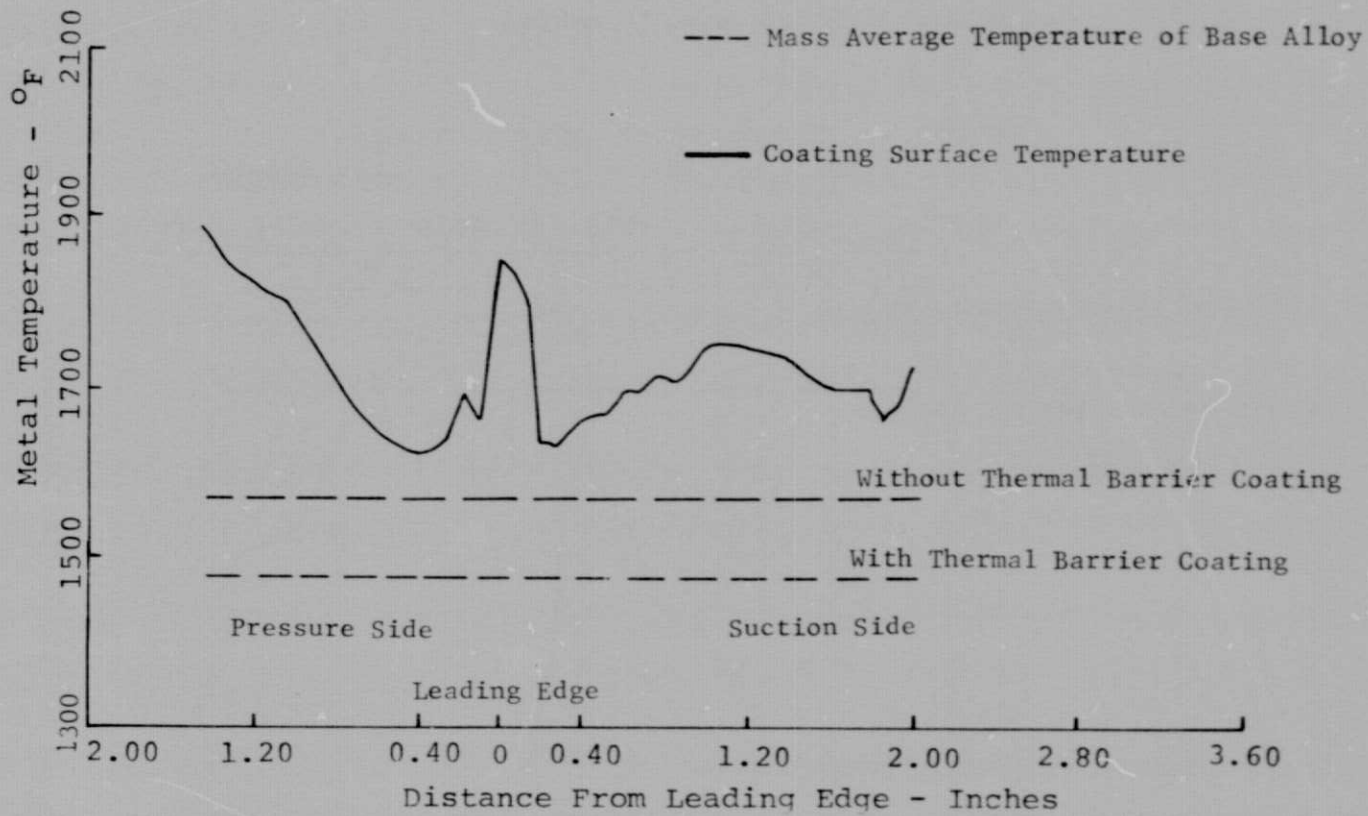


Figure 9. F100(3) Thermal Barrier Coated First-Stage Blade —  
 10% Span, Temperature vs Surface Distribution

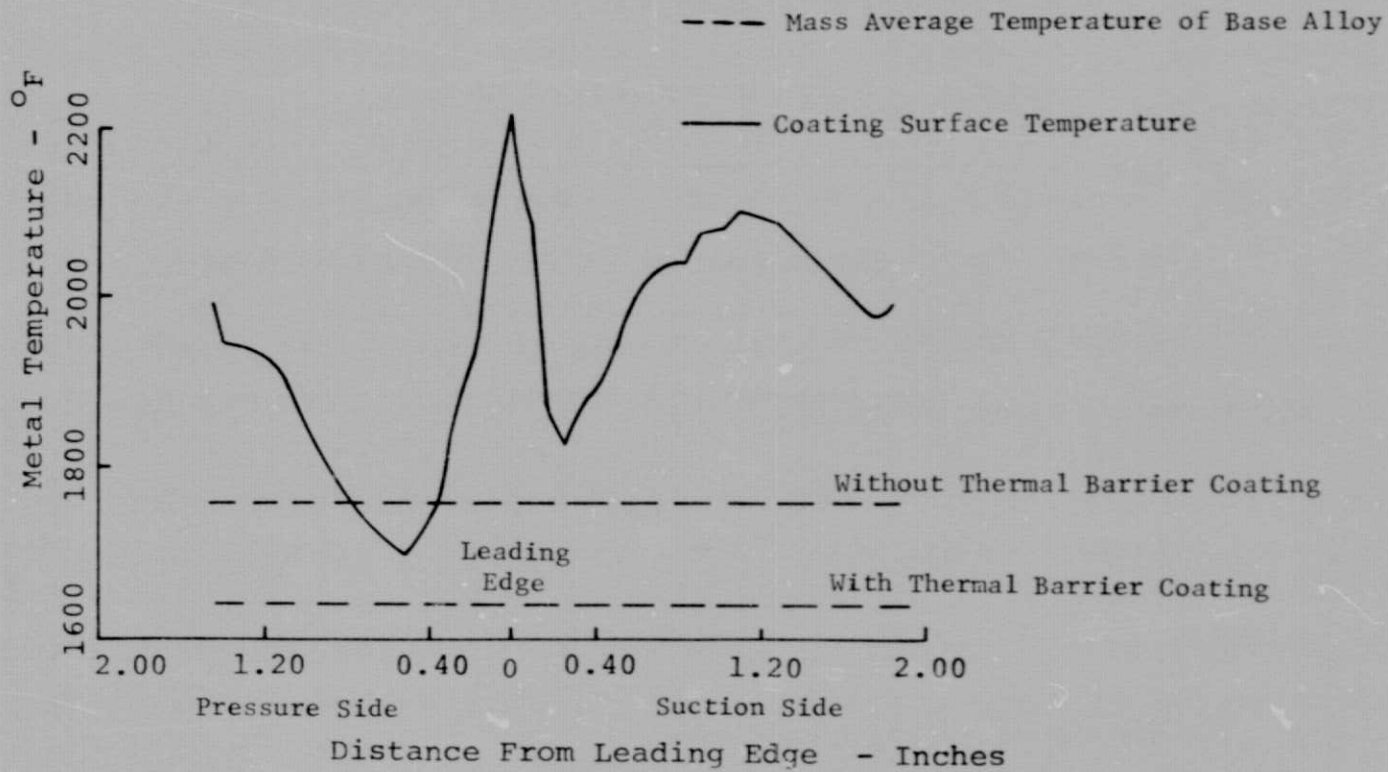


Figure 10. F100(3) Thermal Barrier Coated First-Stage Blade  
 — Midspan, Temperature vs Surface Distribution



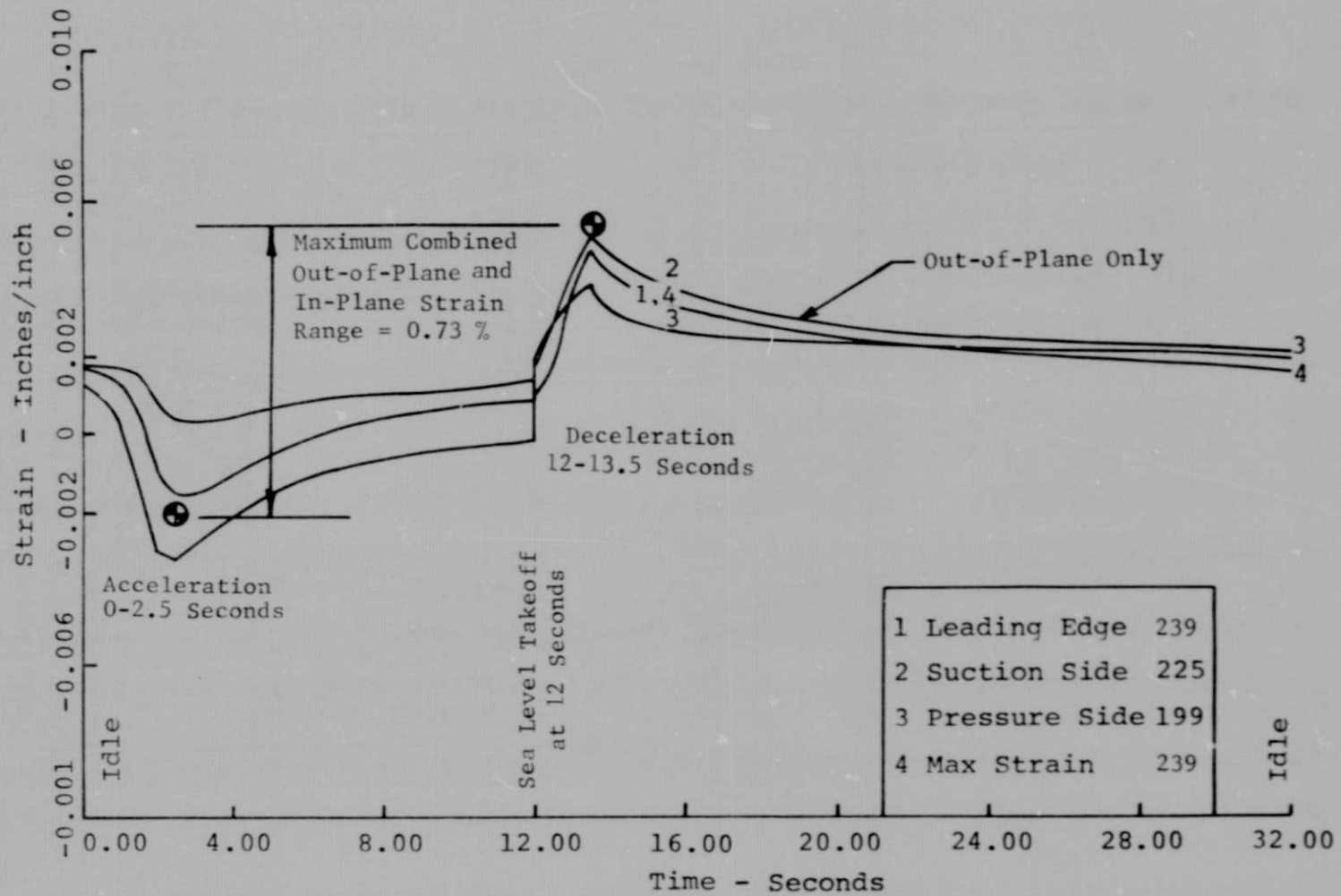


Figure 11. F100(3) Thermal Barrier Coated First-Stage Blade  
— 10% Span, Surface Strain vs Time

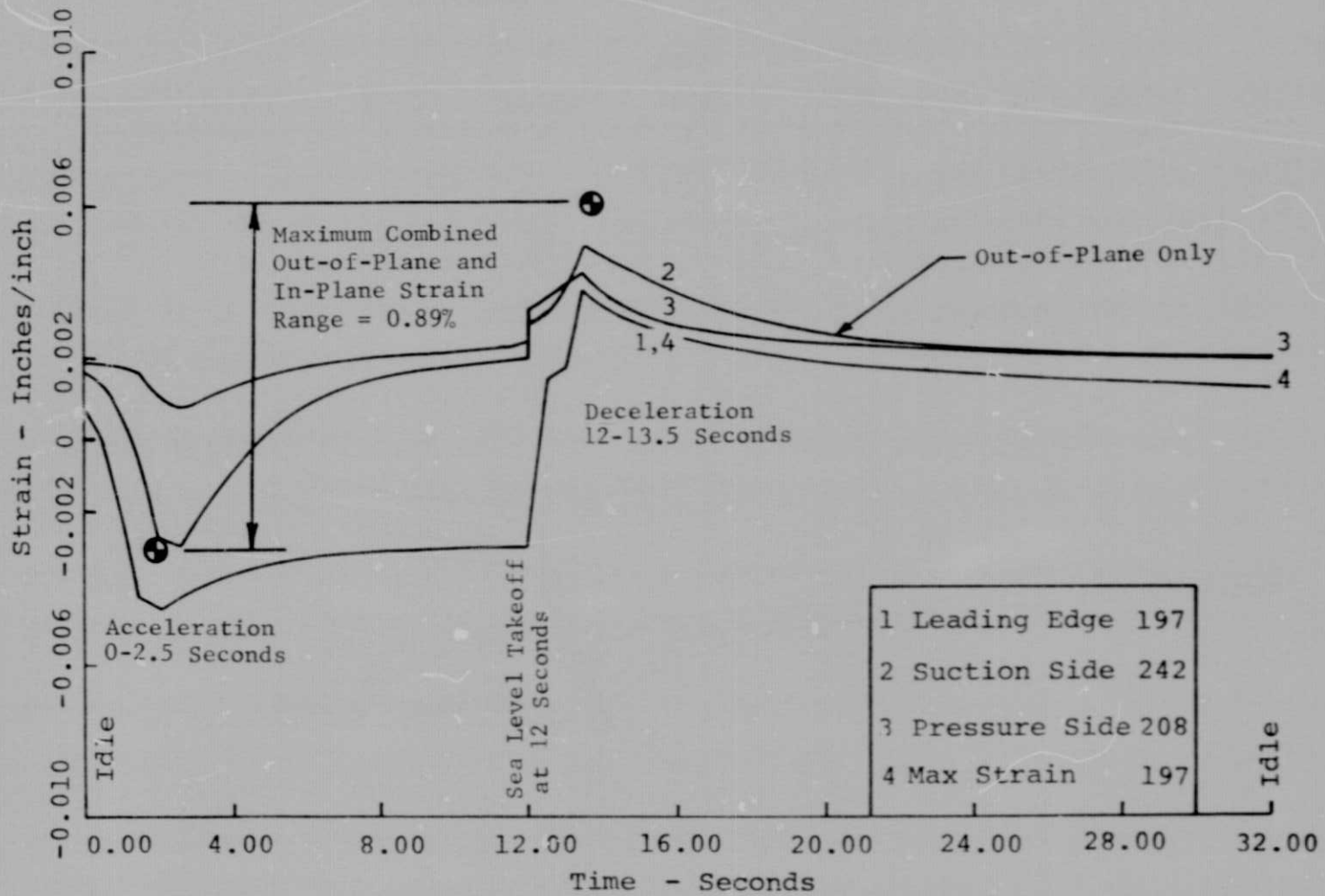


Figure 12. F100(3) Thermal Barrier Coated First-Stage Blade  
— Midspan, Surface Strain vs Time

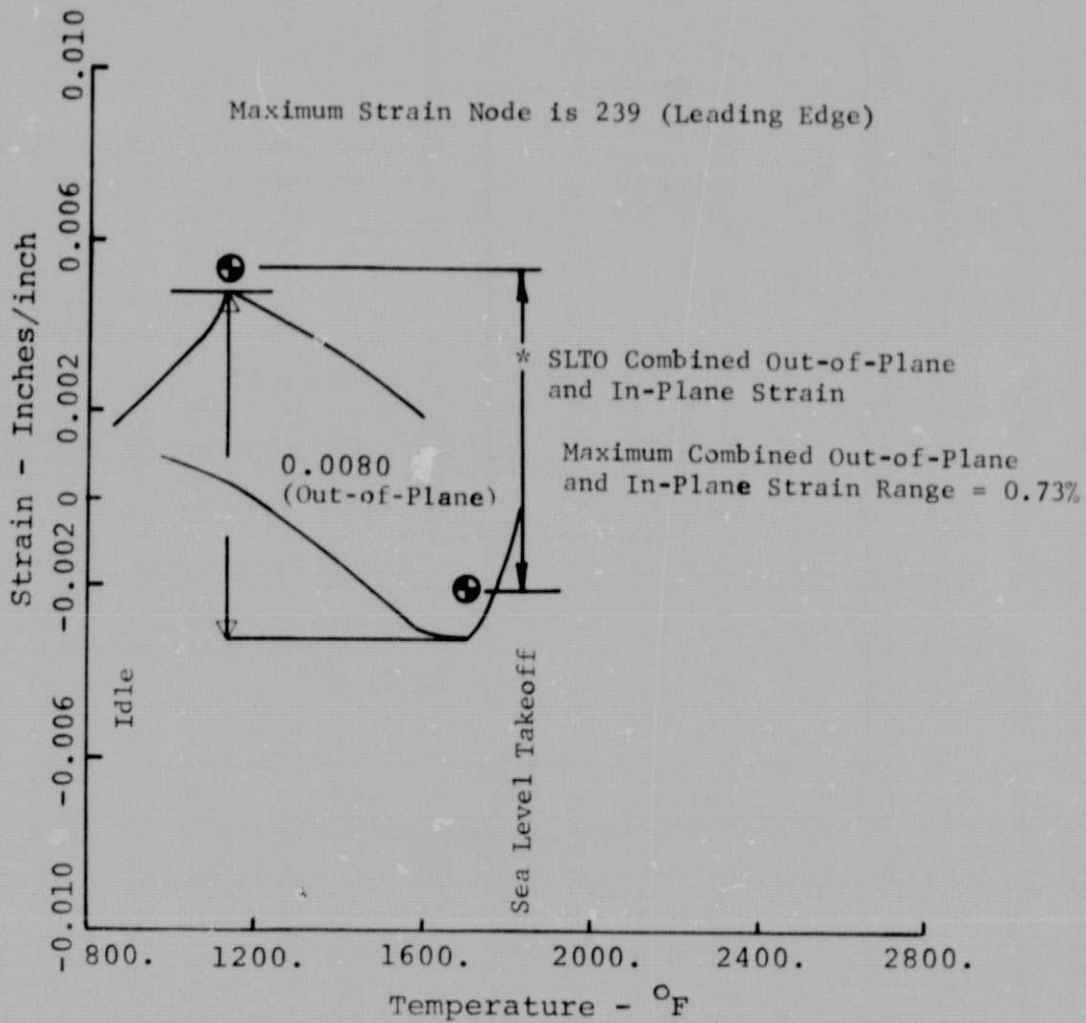


Figure 13. F100(3) Thermal Barrier Coated First-Stage Blade  
— 10% Span, Strain vs Temperature

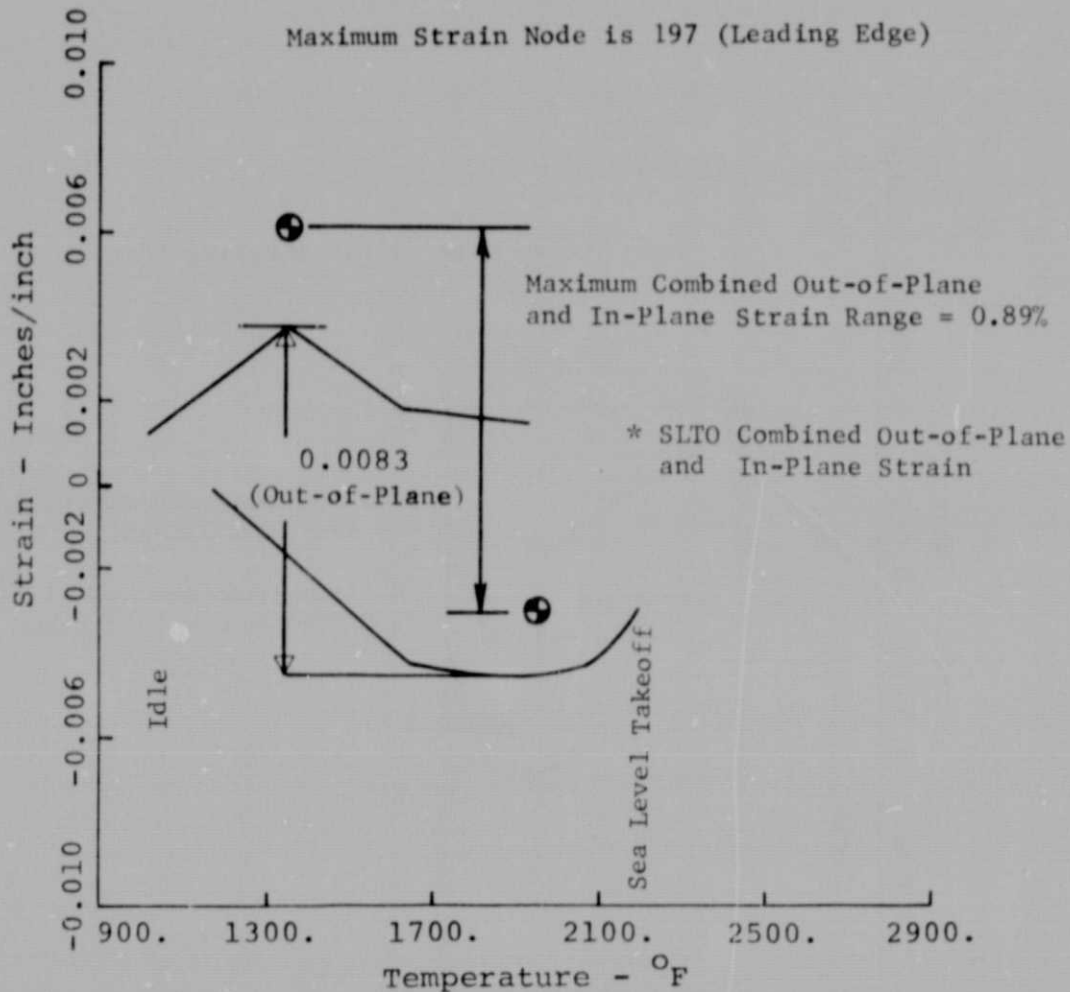


Figure 14. F100(3) Thermal Barrier Coated First-Stage Blade  
— Midspan, Strain vs Temperature

It is more difficult to make a similar judgment relative to TBC survivability or failure. This is primarily the result of insufficient life data for the thermal barrier coating system. The only information currently available is the failure strain data shown in Figure A-5. These data are based on flexure specimens, and represent tensile failures. If these data are used as allowable strains, the predicted values of strain will indicate coating failure essentially all over the airfoil, even when only the tensile portion of the total strain range is used. Obviously this approach is too conservative, since previous experience shows that thermal barrier coatings do survive for short periods of time, and it is mainly the leading edge and pressure side tip-trailing edge quadrant areas that deteriorate in long-term operation. If the coating does fail all over the airfoil, the cracks are not visible to the naked eye. Possibly the stresses in the coating are relieved by micro-cracking, giving the appearance of no damage. Periodic microscopic inspection of the blades would be required to determine the existence and extent of this type of cracking. The design data that is required to make a valid assessment of the calculated results consists of thermal fatigue data (including the effects of steady stress superimposed on alternating stress) for both the elastic and plastic regions of the coating system.

## SECTION V

### CONCLUSIONS AND RECOMMENDATIONS

1. The addition of a 10-mil thermal barrier coating to the F100 first-stage turbine blade resulted in a decrease in average metal temperature of 124°F at midspan. This could be converted into a reduction in first-stage blade cooling air required from 3.59% to 2.40% engine airflow to maintain the same average metal temperature.
2. Maximum surface strain range is increased significantly with the addition of a thermal barrier coating because of the higher thermal gradients across the coated airfoil walls.
3. Based on the failure strain data available, the predicted values of strain would indicate coating failure essentially all over the airfoil. This condition has not been observed on previously-tested parts. It is possible that micro-cracking occurs in the ceramic, thus providing stress relief for the coating while maintaining adhesion to the metal substrate. It is recommended that engine test blades be periodically examined microscopically to determine the existence and extent of this cracking.
4. It is not possible to formulate meaningful conclusions relative to the survivability or failure of the thermal barrier coating without additional material data. It is recommended that a 10-mil thermal barrier coated specimen simulating the FSER blades be lab tested at engine transient conditions to generate applicable coating life data. The specimen should be subjected to the same thermo-mechanical cyclic loading as experienced in the engine.

**APPENDIX**  
**MATERIAL PROPERTIES**

This appendix shows the properties of the various materials used in this analysis for the F100 engine first-stage turbine blades.

- Thermal conductivity vs temperature
- Specific heat vs temperature, density table
- Elastic modulus vs temperature
- Thermal coefficient of linear expansion vs temperature
- Ceramic coating fracture strain vs temperature

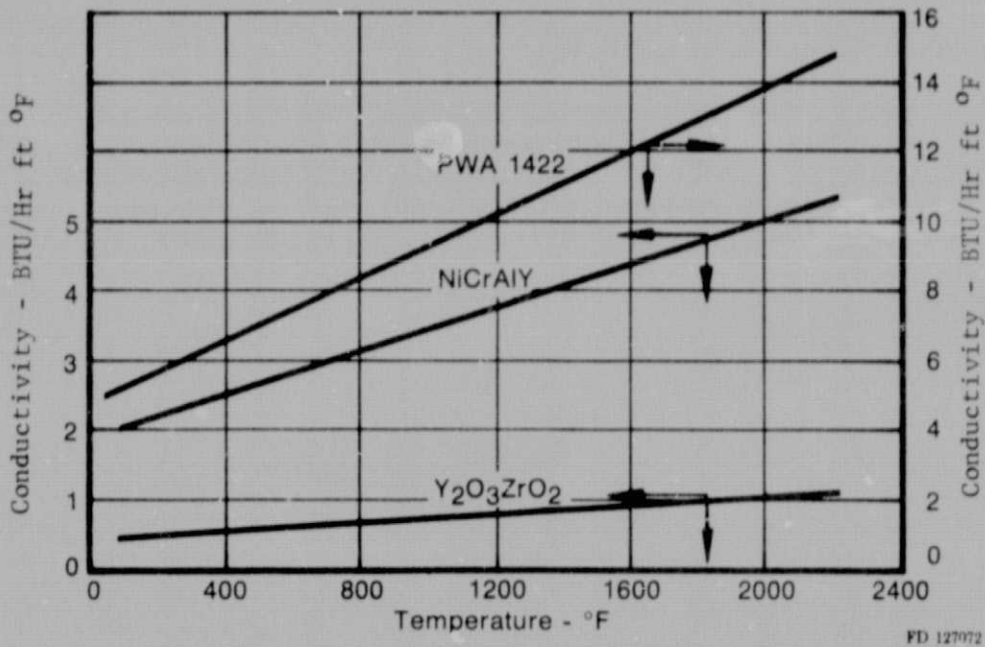
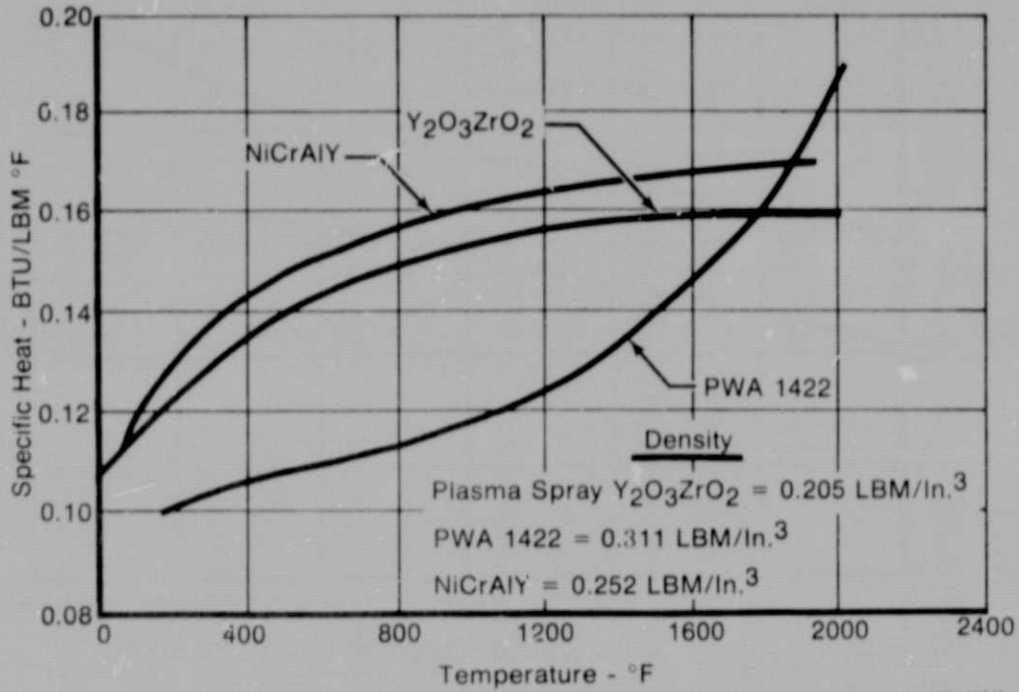


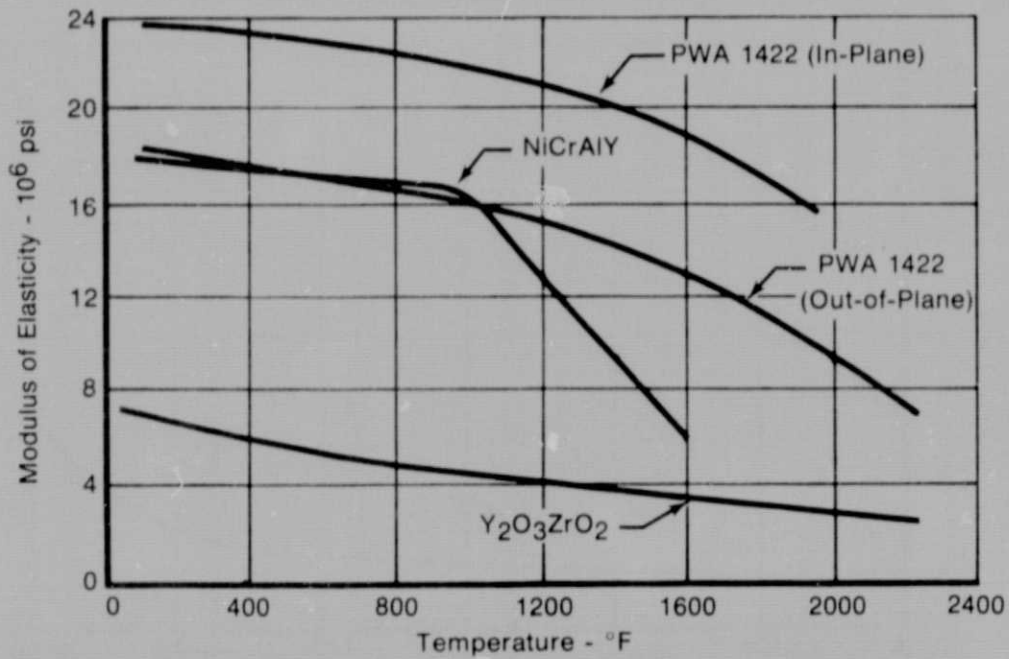
Figure A-1. Thermal Conductivity





FD 127073

Figure A-2. Specific Heat



FD 127071

Figure A-3. Elastic Modulus

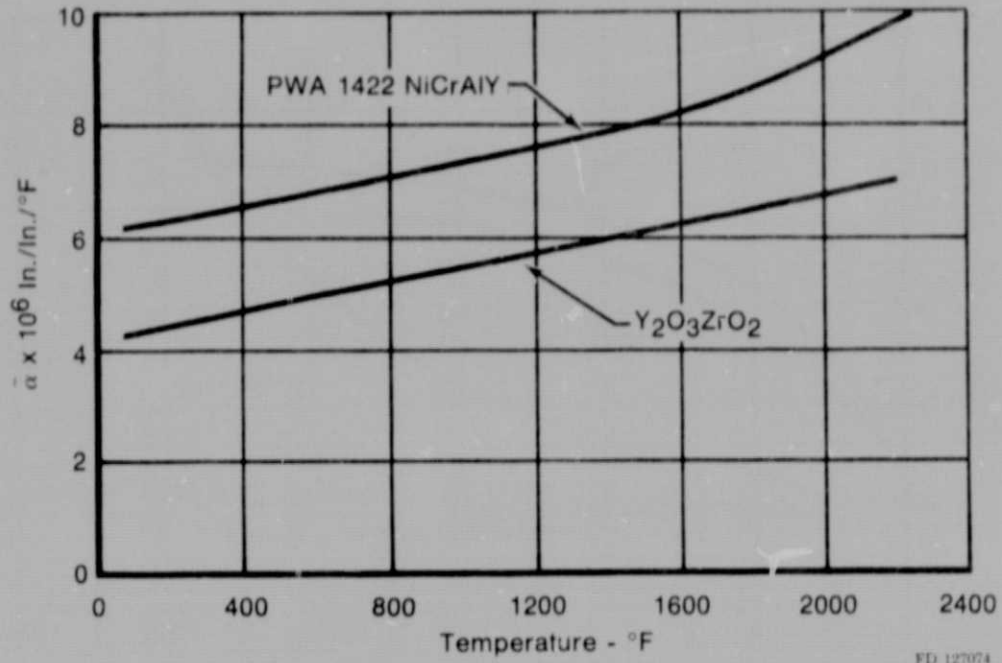


Figure A-4. Thermal Coefficient of Linear Expansion

Reference: P&WA Four Point Bending Tests

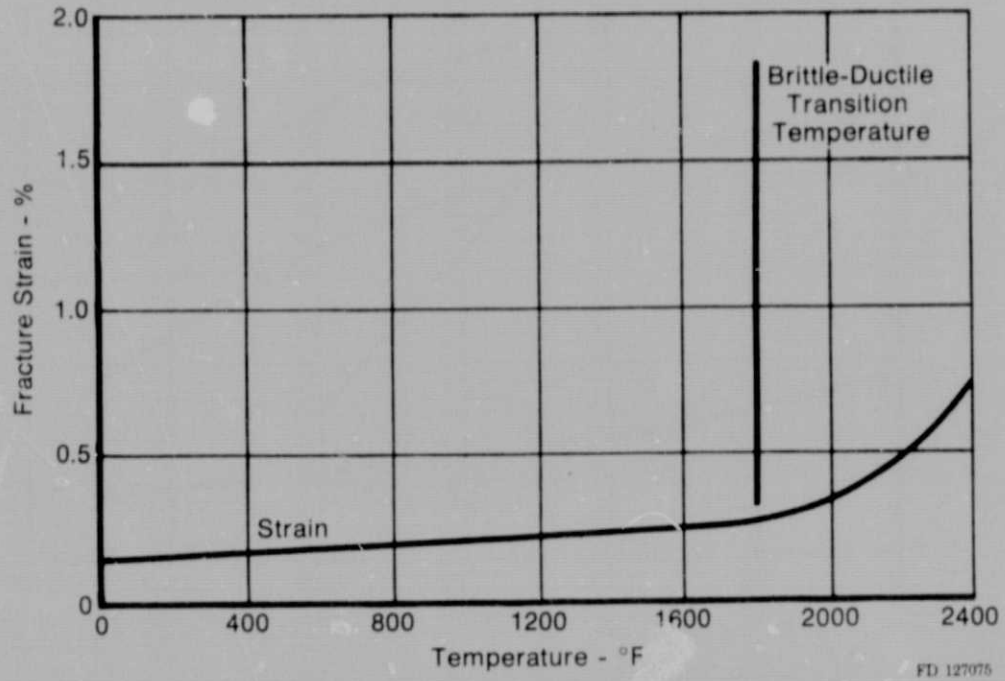


Figure A-5. Ceramic Layer Fracture Strain  
Y₂O₃ZrO₂